Iranian Journal of Medical Physics

ijmp.mums.ac.ir

Evaluation of Contrast to Noise Ratio of Targeted and Non-Targeted Gold nanoparticles in nasopharyngeal cancer cells in CT images

Sara Khademi[1], Hosein Azimian[2], Shabnam Olumi[1], Hossein Ghadiri[3*]

1. Department of Radiology Technology, School of Paramedical and Rehabilitation Sciences, Mashhad University of Medical Sciences, Mashhad, Iran
2. Medical Physics Research Center, Mashhad University of Medical Sciences, Mashhad, Iran
3. Department of Medical Physics and Biomedical Engineering, Tehran University of Medical Sciences, Tehran, Iran

ARTICLE INFO

Article type:
Original Paper

Article history:
Received: Nov 29, 2021
Accepted: Jan 22, 2022

Keywords:
Folic Acid
Molecular Imaging
CT
Gold Nanoparticle
Cancer

ABSTRACT

Introduction: In this study, we aimed to identify the benefits in image contrast enhancement of Folic acid-Cysteamine conjugated gold nanoparticles (FA-Cys-AuNPs) by comparing Contrast to Noise ratio (CNR) of gold nanoparticles (AuNPs) to iodinated compound CT images. The CNR was assessed in different tube voltages, concentrations, and incubation times in nasopharyngeal KB cancer cells.

Material and Methods: FA-Cys-AuNPs and Omnipaque suspension were scanned at different concentration ranges (500-2000 µg/ml) and energy ranges (80- 140 kVp) with CT imaging modality. FA-Cys-AuNPs and AuNPs were incubated in nasopharyngeal cancer cells at different incubation times (6, 12, and 24 h) and concentration ranges (200-500 µM). Finally, the contrast enhancement was assessed using CNR value at different tube voltages.

Results: Results showed that the formed FA-Cys-AuNPs with an Au core size of 15 nm in all concentrations and tube potentials from 80 to 140 kVp display greater CNR than Omnipaque. The CNR value was increased by increasing concentration and energy. At 140 kVp and 2000 µg/ml, the CNR value of FA-Cys-AuNPs was 2.25 times greater than Omnipaque. At 140 kVp, 500 µM and 24 h incubation, the CNR values of targeted cells were approximately 1.5 times higher than non-targeted cells. At 140 kVp, and 500 µM, the CNR value of targeted cells with 24 h incubation time was 2.66 times greater than the targeted cells incubated with 6 h.

Conclusion: These findings suggested that the designed FA-Cys-AuNPs could be a good candidate contrast agent for molecular CT imaging.

► *Please cite this article as:*
Khademi S, Azimian H, Olumi Sh, Ghadiri H. Evaluation of Contrast to Noise Ratio of Targeted and Non-Targeted Gold nanoparticles in nasopharyngeal cancer cells in CT images. Iran J Med Phys 2023; 20: 42-47. 10.22038/IJMP.2022.61916.2046.

Introduction

Molecular Imaging (MI) technique provides to directly or indirectly monitor and record the biological process at the molecular and cellular levels[1]. Among several of MI technologies, Computed Tomography (CT) can afford superior density and spatial resolution to other imaging systems. Furthermore, it is the most generally applied imaging modality in hospitals, cost-effective and it has good deep tissue penetration[2]. For effective CT scanning applications, contrast media are necessary to improve high sensitivity and specificity. To date, iodine-based compounds (e.g., Omnipaque) are used, but it has several disadvantages such as short half time, nephrotoxicity, non-specificity, and non-selected in tumor targeting[3]. To reduce these disadvantages, contrast media must have a high atomic number and electron density, easy control of the size, biocompatibility and must be targeted to increase sensitivity[4]. Recent studies indicated that nanotechnology using increasing the sensitivity of images can be used in MI technologies. In particular, gold nanoparticles (AuNPs) are preferred rather than iodine-base contrast agents due to; their high atomic number (Z=79), and high electron density that leads to a strong X-ray attenuation coefficient. Furthermore, AuNPs are reported to be biocompatible in determined concentration ranges and easily tunable surface modification with functional ligands such as specific biomarkers, peptides, antibodies, and folic acid (FA) or folate for the specific goal of MI applications [5-8]. Finally, the suitable surface modifying can help AuNPs to reduce elimination using the reticuloendothelial system (RES); therefore, it can prolong half-time and circulation time[9]. Specific targeting method or active targeting means to the accumulation of targeted contrast media because of the use of adhesion ligands at a specific site. One promising active and specific targeting method is utilized using folic acid (C_{19} H_{19} N_7 O_6 (Mw=441.4 Da). The FA is water-soluble and exists in cancer and

*Corresponding Author: Tel: +98-09154777256; Email: h-ghadiri@sina.tums.ac.ir

normal cells because of its FA-receptor. FA is mainly protected by immune system in normal cells, but is exposed largely expressed in different cancer cells, including nasopharyngeal [8, 10-12]. It overexpresses of FR vitamin on cancer cells rather than normal cells and its feasible conjugation with AuNPs can be used to be actively targeted with FA-linked imaging[12]. In this study, Cysteamine was used as a linker to easily attach to AuNPs because of the presence of –SH (thiol group), and non-toxicity. In our previous studies, the cytotoxicity of folic acid conjugation AuNPs through cysteamnie (FA-Cys-AuNPs) was evaluated using colony and MTT assay, Flow cytometry for evaluating cell cycle and apoptosis, and Hematoxylin-Eosin (H&E) stain in both in vitro and in vivo studies[6, 13]. The characterization of NPs was done using Transmission electron microscopy (TEM), Dynamic Light Scattering (DLS), UV-visible, and Fourier-transform infrared spectroscopy (FTIR) analyses. The X-ray attenuation intensity of targeted and non-targeted of NPs was measured in various concentrations, X-ray tube voltages, and incubation times [6, 13]. In the present study, we studied the contrast enhancement using contrast to noise ratio (CNR) value at different concentrations, incubations times and X-ray energy tube for both FA-Cys-AuNPs and AuNPs. Finally, the CNR value of targeted NPs was compared with iodine based contrast media (Omnipaque) at the same concentration and X-ray tube potential. Based on our knowledge, it is the first study that evaluated the CNR value of targeted AuNPs versus non-targeted AuNPs at various concentrations, X-ray tube potential, and incubation time.

Materials and Methods

Materials

In the previous study, we synthesized and characterized FA-Cys-AuNPs and AuNPs[6]. Transmission electron microscopy (TEM) was done (Zeiss EM 900, Germany) to assess the size and shape of the FA-Cys-AuNPs and AuNPs. Dynamic Light Scattering (DLS) was used to determine the hydrodynamic size of NPs. The concentration of NPs was determined by inductively coupled plasma optical emission spectrometry (ICP-OES). UV-visible was done by a SPEKOL 2000 (JENA, UK) spectrophotometer. In the previous study, the cytotoxicity of NPs was done using colony and MTT assays, Flow cytometry for evaluating cell cycle and apoptosis, and Hematoxylin-Eosin (H&E) stain. KB cells were acquired from Pasteur Institute in Tehran, Iran.

Contrast to Noise Ratio (CNR) value of FA-Cys-AuNPs versus AuNPs in KB cancer cells

The density of 1×10^6 KB cells/well were seeded in 6-well plates[6]. After that, the KB cells were incubated with targeted and non-targeted AuNPs at the concentration of (0-500 µM) for 6, 12, and 24 h at 5 % CO_2 and 37 ^{0}C. Afterwards, the cells were washed three times with PBS and trypsinized, and suspended in 0.5 ml Eppendorf vial and placed into polymethylmetacrylic (PMMA) phantom. The vials were imaged using a CT imaging modality (GE Light Speed VCT 64 slice CT scanner) by the parameter of: Peak kilovoltages of 80, 100, 120, and 140kVp; pitch 1; slice thickness: 0.625 mm; tube current time: 200 mAs, and display field of view: 130×130 mm. The CNR value of FA-Cys-AuNPs was compared with AuNPs nanoparticles at different concentrations, X-ray tube potentials, and incubation times.

Contrast to Noise Ratio (CNR) value of FA-Cys-AuNPs versus Omnipaque in phantom

The CNR value of FA-Cys-AuNPs and iodine-based contrast agent (Omnipaque 300 mg/ml) solutions were evaluated with various concentrations (250, 500, 1000, 1500, and 2000 µg/ml) in a 0.5 ml Eppendorf vial that placed in a self-designed phantom (made of PMMA). The vials were imaged using a CT imaging modality (GE Light Speed VCT 64 slice CT scanner) by the parameter of: Peak kilovoltages of 80, 100, 120, and 140kVp; pitch 1; slice thickness: 0.625 mm; Tube current time: 200 mAs, and display field of view: 130×130 mm.

Image and statistical analysis

After CT imaging, Images were loaded to standard software (DICOM viwer :Medixant company, Poland) and analyzed by placing a uniform circular region of interest (ROI) and obtaining an attenuation value in the mean Hounsfield Units (HU) in three slices in each vial (three samples in each concentration). The mean HU values and standard deviations were recorded for both AuNPs and Omnipaque at each concentration, X-ray tube potentials, and incubation times. The noise was defined as the standard deviation of the ROI pixels in the water region. Contrast to Noise Ratio (CNR) was calculated from the recorded HU using plotting the ROI analysis across the images[14]. The CNR formula was calculated via the following equation:

$$\mathrm{CNR} = \frac{(\boldsymbol{Attentaion\ (sample) - Attentaion\ (water)})}{\boldsymbol{Noise}} \quad (1)$$

Statistical analysis was done using SPSS software version 22. One-way analysis of variance and Tukey's multiple comparison tests were used to assess the significance of the data. A P-value less than 0.05 was considered statistically significant.

Results

CNR property of the FA-Cys-AuNPs versus Omnipaque in phantom

The Contrast to Noise Ratio (CNR) value of the formed FA-Cys-AuNPs was compared with an iodine-based small molecular CT contrast agent at different concentrations of elements and X-ray tube potentials. , The axial CT images of FA-Cys-AuNPs and conventional iodine-based is shown in Fig. 1 (A). By increasing of Au or iodine molecules concentration, the CT images brightness is increased[6]. In Fig. 1 (B) the CNR value of both FA-Cys-AuNPs and

conventional iodine-based is increased by increasing in concentration from 500 to 2000 µg/ml. however, the increasing trend of targeted NPs is higher in CNR value than that of Omnipaque at the same concentration. At 140 kVp and 2000 µg/ml, the CNR value of FA-Cys-AuNPs is approximately 2.25–times higher than that of iodine-based molecular contrast agent. At 140 kVp and 1500 µg/ml, the CNR value of FA-Cys-AuNPs is approximately 1.75–times higher than that of iodine-based molecular contrast agent. At 140 kVp and 1000 µg/ml, the CNR value of FA-Cys-AuNPs is approximately1.66–times higher than that of iodine-based molecular contrast agent. At 140 kVp, the CNR value of targeted NPs at 2000 µg/ml was found to be approximately 4.5-times higher than the CNR value at 500 µg/ml. At 140 kVp, the CNR value of Omnipaque at 2000 µg/ml was found to be approximately 4-times higher than the CNR value at 500 µg/ml.

In Figure 2, the CNR value of FA-Cys-AuNPs is compared with Omnipaque at different X-ray energies. As shown in Fig. 2, the CNR value of both targeted NPs and iodine-based molecular contrast agents is increased by increasing in X-ray tube potential from 80 to 140 kVp. At 140 kVp and 2000 µg/ml, the CNR value of FA-Cys-AuNPs is approximately 2.25–times higher than that of an iodine-based molecular contrast agent. At 120 kVp and 2000 µg/ml, the CNR value of FA-Cys-AuNPs is approximately2–times higher than that of iodine-based molecular contrast agent. At 80 kVp and 2000 µg/ml, the CNR value of FA-Cys-AuNPs is approximately1.88–times higher than that of iodine-based molecular contrast agent. At 2000 µg/ml, the CNR value of targeted NPs at 140 kVp was found to be approximately 2.64-times higher than the CNR value of targeted NPs at 80 kVp. At 2000 µg/ml, the CNR value of targeted NPs at 120 kVp was found to be approximately 1.76-times higher than the CNR value of targeted NPs at 80 kVp. At 2000 µg/ml, the CNR value of Omnipaque at 140 kVp was found to be approximately 2.22-times higher than the CNR value of Omnipaque at 80 kVp. At higher kVp, the CNR value was increased at higher concentration ranges.

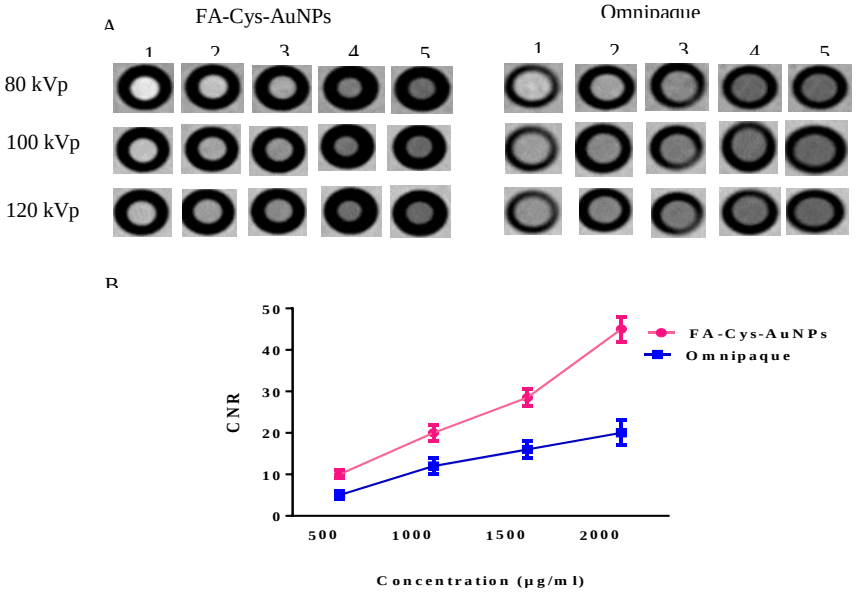

Figure 1. A) CT images of FA-Cys-AuNPs and Omnipaque at different X-ray tube potentials (80, 100, and 120 kVp) and at the different concentrations of 1:2000 (µg/ml), 2: 1500 (µg/ml), 3: 1000 (µg/ml), 4:500 (µg/ml), 5: 250 (µg/ml). B). The CNR value of FA-Cys-AuNPs versus Omnipaque at different concentrations (500, 1000, 1500, and 2000 (µg/ml)) and the X-ray tube potential of 140 kVp.

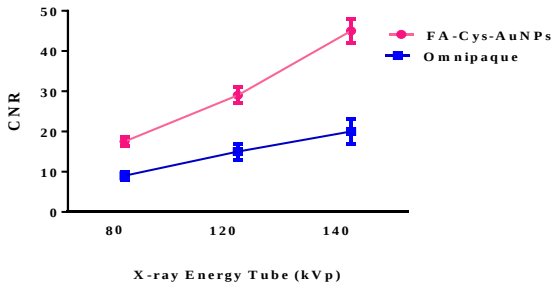

Figure 2. The CNR value of FA-Cys-AuNPs versus Omnipaque at different X-ray tube potentials (80, 120, and 140 kVp) and the concentration of 2000 µg/ml.

CNR property of the FA-Cys-AuNPs versus AuNPs in nasopharyngeal cancer cells

In this study, we assessed the possibility to apply the complex of FA-Cys-AuNPs for molecular CT imaging of KB cells. The nasopharyngeal cancer cells were incubated with targeted and non-targeted nanocomples at various concentrations (0-500 µM) and incubation times (6, 12, and 24 h). The samples were scanned using a CT imaging system at various X-ray tube potentials (80, 100, 120, and 140 kVp). The CNR value was measured at different concentrations, X-ray tube potentials, and concentrations of NPs. As shown in Fig. 3, the CNR value is increased by increasing in the concentration of both targeted and non-targeted NPs. At 140 kVp, 500 µM, and 24 h incubation, the CNR value of targeted NPs is approximately 1.5-times rather than of non-targeted cells ($P<0.05$). At 140 kVp, 500 µM, and 12 h incubation, the CNR value of targeted NPs is approximately 1.6-times rather than non-targeted cells. At 140 kVp, 500 µM, and 6 h incubation, the CNR value of targeted NPs is approximately 1.5-times rather than non-targeted cells. At 500 µM, the CNR value of targeted NPs at 24 and 12 h incubation time was found to be approximately 2.66-times and 2-times higher than the CNR value of targeted AuNPs at 6 h incubation time, respectively. At 500 µM, the CNR value of non-targeted AuNPs at 24 and 12 h incubation time was found to be approximately 2.8-times and 2-times higher than the CNR value of non-targeted AuNPs at 6 h incubation time, respectively. At 500 µM, the CNR value of targeted NPs at 24 h incubation time was found to be approximately 1.25–times and 2.66-times higher than the CNR value of targeted AuNPs at 12 and 6 h incubation time, respectively. The highest CNR value was obtained at higher concentration and incubation time in targeted AuNPs.

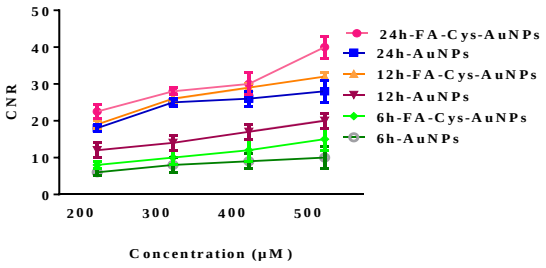

Figure 3. The CNR value of KB cells incubated with FA-Cys-AuNPs and AuNPs at different concentrations (200, 300, 400, and 500 µM), incubation times (6, 12, and 24 h), and at the tube voltage of 140 kVp.

Figure 4, shows obtained CNR value of targeted AuNPs and non-targeted AuNPs as a function of X-ray tube potentials and incubation times. By increasing the X-ray tube potentials and incubation time, the CNR value increases for both targeted and non-targeted AuNPs. The highest CNR value was obtained for targeted AuNPs at 140 kVp and 24 h incubation time ($P<0.05$). At 140 kVp, and 24 h incubation, the CNR value of targeted AuNPs is approximately 1.66 and 2.66-times higher than 12 and 6 h incubation times, respectively. At 120 kVp, and 24 h incubation, the CNR value of targeted AuNPs is approximately 1.13 and 1.92-times higher than 12 and 6 h incubation times, respectively. At 100 kVp, and 24 h incubation, the CNR value of targeted AuNPs is approximately 1 and 1.66-times higher than 12 and 6 h incubation times, respectively. At 80 kVp, and 24 h incubation, the CNR value of targeted AuNPs is approximately 1.28 and 1.8-times higher than 12 and 6 h incubation times, respectively.

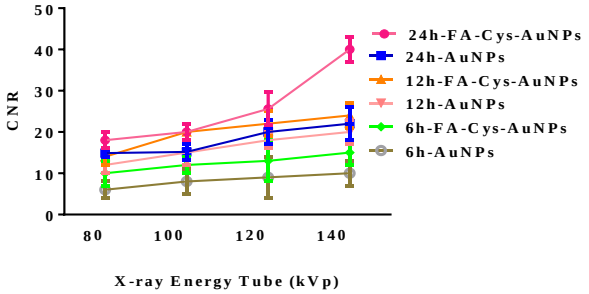

Figure 4. The CNR value of KB cells incubated with FA-Cys-AuNPs and AuNPs at different X-ray tube voltage (80, 100, 120, and140 kVp), incubation times (6, 12, and 24 h), and at the concentration of 500 µM.

Discussion

In this study, we have shown that FA-Cys-AuNPs have a greater CNR than conventional iodine-based contrast media (Omnipaque) at different concentrations and X-ray tube potentials. The CNR value of both FA-Cys-AuNPs and conventional iodine-based were increased by increasing in concentration. However, the increasing trend of FA-Cys-AuNPs was higher in CNR value than that of Omnipaque at the same concentration. At 140 kVp and 2000 µg/ml, the CNR value of FA-Cys-AuNPs was approximately 2.25–times higher than that of an iodine-based molecular contrast agent. Furthermore, it was found that the CNR value of targeted NPs at 140 kVp was found to be approximately 2.64-times higher than the CNR value of targeted NPs at 80 kVp. Theoretically, gold nanoparticles have a higher X-ray attenuation coefficient than Omnipaque because of higher atomic number ($Z=79$) versus ($Z=53$) and electron density (19.32 g/cm^3) versus (4.9 g/cm^3) rather than iodine-based contrast media[15]. The photoelectric absorption effect (PAE) is mainly dependent on the atomic number of materials that interacted with X-ray photons that are proportional to Z^4[8] .These results propose higher CNR value of the targeted AuNPs than that of iodine-based contrast media is important for an excellent-sensitivity X-ray imaging application. Several studies have revealed the highest CT contrast enhancement of AuNPs versus conventional iodine-based contrast media. Jackson et al[16]. evaluated the CNR value of AuNPs and iodine contrast media at different concentrations and X-ray tube potentials. Their results indicated that by increasing kVp the contrast enhancement of both contrast media was increased.

Their results indicated that the CNR value for AuNPs was approximately 114% higher than iodine-based contrast media at the X-ray tube potential of 140 kVp. Galper et al[17]. revealed that the CNR value of AuNPs was nearly 1.9 times greater than the iodine-based contrast agent at the X-ray tube potential of 120 kVp. Harun et al[14]. showed that AuNPs at the size of 1.9 and 15 nm and iodine contrast media had the highest CNR at 140 kVp. The best interaction of X-ray energy happened at the higher K-edge value. Kim et al [18]. evaluated the CNR value of polyethylene glycol (PEG)-AuNPs versus iodine-based contrast media in the range of 1-3 M. Their results indicated that the CNR value of AuNPs was 1.9 times greater than iodine contrast media (Ultravist). Our findings agree with all the above-mentioned research.

AuNPs and FA-Cys-AuNPs suspensions were synthesized and characterized in the current study.

The CNR values of AuNPs and FA-Cys-AuNPs were evaluated at different concentrations, incubation times and kVp. At 140 kVp, and 24 h incubation, the CNR value of targeted AuNPs is approximately 1.66 and 2.66-times higher than 12 and 6 h incubation times, respectively. The highest CNR value was obtained at higher concentration, incubation time, and X-ray tube potential. Due to the ability of active targeting of FA, the contrast media increased in the cancer cells in contrast to the normal cells, and the uptake of cells was increased at a higher concentration range of NPs[3]. The nasopharyngeal cancer cells treated with FA-Cys-AuNPs revealed a higher CNR value than those incubated with the AuNPs at the same concentration, X-ray tube potential, and incubation time. With the increase in the incubation time of AuNPs with nasopharyngeal cancer cells, the mass of AuNPs gradually increased. Recently, the use of FA targeting has been assessed in cancer diagnosis. For example, HU et al[19]. evaluated the multifunctional FA-Fe_3O_4@Au NPs for targeted Magnetic Resonance Imaging (MRI) and CT imaging. The TEM analysis was applied to evaluate the targeting potential of the NPs to the Hella cells. Their results indicated that higher X-ray attenuation of the Hella cells was attributed to the higher cellular uptake of FA conjugated NPs in cancer cells overexpressing higher FA receptors. These findings suggest that FA as the targeting molecule, can much uptake of AuNPs due to bindings with FA receptors on the surface of nasopharyngeal cancer cells. Therefore, its property led to a higher CNR value than non-targeted AuNPs cells in CT images. It must be mentioned that these results were obtained by hospital CT imaging, that it has a low resolution (0.625 mm) compared to micro (μ)-CT (45 μm), therefore because of μ-CT has not been practically used in the clinic, these results have a good potential for hospital applications.

Conclusion

Through this study, we have shown that utilizing gold nanoparticles with great X-ray attenuation properties in conjugated with folic acid targeting presented a CT-based molecular probe and suggested a targeted CT scanning strategy for specific diagnosis of cancer cells. Attachment of FA augmented the AuNPs accumulation in the nasopharyngeal cancer cells in comparison to the non-targeted cells due to the active targeting capability of FA. Our results showed that nasopharyngeal cancer cells can be detected under CT scanning after incubation with the FA-Cys-AuNPs in vitro. The CNR value is strongly dependent on concentration, active targeting, incubation time of (AuNPs) and X-ray tube potential. The higher CNR property of FA-Cys-AuNPs than that of AuNPs enables effective targeted imaging of KB cells under the same concentration contrast agent and a higher CNR value was provided using FA-Cys-AuNPs compared to Omniapque. With the facile Cysteamine nanotechnology and surface conjugation chemistry properties, different active targeted AuNPs-Cysteamine could be synthesized for actively targeted imaging of various types of tumor cells. In our future endeavor, the CNR value of in vivo study and radiation dose enhancement will be evaluated.

Acknowledgment

S.Kh and H.A contributed equally to this work. This research was financially supported by Tehran University of Medical Sciences, Tehran, Iran. (Grant (No: 30853)).

References

1. Lalumera, E., S. Fanti, and G. Boniolo, Reliability of molecular imaging diagnostics. Synthese, 2021 Oct; 198(23): p. 5701-5717.
2. Keshtkar, M., D. Shahbazi-Gahrouei, and A. Mahmoudabadi, Synthesis and application of Fe3O4@ Au composite nanoparticles as magnetic resonance/computed tomography dual-modality contrast agent. JMSS, 2020Jul; 10(3): p. 201.
3. Shakeri-Zadeh A, Rezaeyan A, Sarikhani A, Ghaffari H, Samadian H, Khademi S, Ghaznavi H, Bulte JW. Folate receptor-targeted nanoprobes for molecular imaging of cancer: Friend or foe? Nano Today. 2021 Aug 1;39:101173
4. Khademi S, Shakeri-Zadeh A, Solgi R, Azimian H, Ghadiri H. Observation of targeted gold nanoparticles in nasopharyngeal tumour nude mice model through dual-energy computed tomography. IET Nanobiotechnology, 2021 Sep;15(7):594-601..
5. Ghaznavi H, Hosseini-Nami S, Kamrava SK, Irajirad R, Maleki S, Shakeri-Zadeh A, Montazerabadi A. Folic acid conjugated PEG coated gold–iron oxide core–shell nanocomplex as a potential agent for targeted photothermal therapy of cancer. Artificial cells, nanomedicine, and biotechnology. 2018 Nov 17;46(8): p.1594-604.
6. Khademi S, Sarkar S, Shakeri-Zadeh A, Attaran N, Kharrazi S, Ay MR, Ghadiri H. Folic acid-cysteamine modified gold nanoparticle as a nanoprobe for targeted computed tomography imaging of cancer cells. Materials Science and Engineering: C. 2018 Aug 1;89:182-93.
7. Beik, J., et al., A nanotechnology-based strategy to increase the efficiency of cancer diagnosis and therapy: folate-conjugated gold nanoparticles. Curr.

Med. Chem, 2017. 24(39): p. 4399-4416. Beik J, Khademi S, Attaran N, Sarkar S, Shakeri-Zadeh A, Ghaznavi H, Ghadiri H. A nanotechnology-based strategy to increase the efficiency of cancer diagnosis and therapy: folate-conjugated gold nanoparticles. Current medicinal chemistry. 2017 Dec 1;24(39):4399-416.

8. 8. Beik, J., et al., The benefits of folic acid-modified gold nanoparticles in CT-based molecular imaging: radiation dose reduction and image contrast enhancement. Artif Cells Nanomed Biotechnol, 2018. 46(8): p. 1993-2001. Beik J, Jafariyan M, Montazerabadi A, Ghadimi-Daresajini A, Tarighi P, Mahmoudabadi A, Ghaznavi H, Shakeri-Zadeh A. The benefits of folic acid-modified gold nanoparticles in CT-based molecular imaging: radiation dose reduction and image contrast enhancement. Artificial cells, nanomedicine, and biotechnology. 2018 Nov 17;46(8):1993-2001.
9. Fan Y, Tu W, Shen M, Chen X, Ning Y, Li J, Chen T, Wang H, Yin F, Liu Y, Shi X. Targeted tumor hypoxia dual-mode CT/MR imaging and enhanced radiation therapy using dendrimer-based nanosensitizers. Advanced Functional Materials. 2020 Mar;30(13):1909285.
10. Montazerabadi, A., et al., Folate-modified and curcumin-loaded dendritic magnetite nanocarriers for the targeted thermo-chemotherapy of cancer cells. Artif Cells Nanomed Biotechnol, 2019. 47(1): p. 330-340. Montazerabadi A, Beik J, Irajirad R, Attaran N, Khaledi S, Ghaznavi H, Shakeri-Zadeh A. Folate-modified and curcumin-loaded dendritic magnetite nanocarriers for the targeted thermo-chemotherapy of cancer cells. Artificial cells, nanomedicine, and biotechnology. 2019 Dec 4;47(1):330-40.
11. Zeinizade, E., et al., Selective apoptosis induction in cancer cells using folate-conjugated gold nanoparticles and controlling the laser irradiation conditions. Artif Cells Nanomed Biotechnol, 2018. 46(sup1): p. 1026-1038. Zeinizade E, Tabei M, Shakeri-Zadeh A, Ghaznavi H, Attaran N, Komeili A, Ghalandari B, Maleki S, Kamrava SK. Selective apoptosis induction in cancer cells using folate-conjugated gold nanoparticles and controlling the laser irradiation conditions. Artificial cells, nanomedicine, and biotechnology. 2018 Oct 31;46(sup1):1026-38.
12. Movahedi, M.M., et al., Investigating the photo-thermo-radiosensitization effects of folate-conjugated gold nanorods on KB nasopharyngeal carcinoma cells. Photodiagnosis and photodynamic therapy, 2018. 24: p. 324-331. Movahedi MM, Mehdizadeh A, Koosha F, Eslahi N, Mahabadi VP, Ghaznavi H, Shakeri-Zadeh A. Investigating the photo-thermo-radiosensitization effects of folate-conjugated gold nanorods on KB nasopharyngeal carcinoma cells. Photodiagnosis and Photodynamic Therapy. 2018 Dec 1;24:324-31.
13. Khademi, S., et al., Targeted gold nanoparticles enable molecular CT imaging of head and neck cancer: an in vivo study. The international journal of biochemistry & cell biology, 2019. 114: p. 105554. Khademi S, Sarkar S, Shakeri-Zadeh A, Attaran N, Kharrazi S, Ay MR, Azimian H, Ghadiri H. Targeted gold nanoparticles enable molecular CT imaging of head and neck cancer: an in vivo study. The international journal of biochemistry & cell biology. 2019 Sep 1;114:105554.
14. Harun, A.Z., et al., Evaluation of Contrast-Noise Ratio (CNR) in contrast enhanced CT images using different sizes of gold nanoparticles. Mater. Today: Proc., 2019. 16: p. 1757-1765. Harun AZ, Ab Rashid R, Ab Razak K, Geso M, Rahman WN. Evaluation of contrast-noise ratio (CNR) in contrast enhanced CT images using different sizes of gold nanoparticles. Materials Today: Proceedings. 2019 Jan 1;16:1757-65.
15. Khademi, S., et al., Evaluation of size, morphology, concentration, and surface effect of gold nanoparticles on X-ray attenuation in computed tomography. Physica Medica, 2018. 45: p. 127-133. Khademi S, Sarkar S, Kharrazi S, Amini SM, Shakeri-Zadeh A, Ay MR, Ghadiri H. Evaluation of size, morphology, concentration, and surface effect of gold nanoparticles on X-ray attenuation in computed tomography. Physica Medica. 2018 Jan 1;45:127-33.
16. Jackson, P.A., et al., Potential dependent superiority of gold nanoparticles in comparison to iodinated contrast agents. Eur. J. Radiol., 2010. 75(1): p. 104-109. Jackson PA, Rahman WN, Wong CJ, Ackerly T, Geso M. Potential dependent superiority of gold nanoparticles in comparison to iodinated contrast agents. European journal of radiology. 2010 Jul 1;75(1):104-9.
17. Kim, J., et al., Use of nanoparticle contrast agents for cell tracking with computed tomography. Bioconjugate chemistry, 2017. 28(6): p. 1581-1597 Kim J, Chhour P, Hsu J, Litt HI, Ferrari VA, Popovtzer R, Cormode DP. Use of nanoparticle contrast agents for cell tracking with computed tomography. Bioconjugate chemistry. 2017 Jun 21;28(6):1581-97..
18. Kim, D., et al., Antibiofouling polymer-coated gold nanoparticles as a contrast agent for in vivo X-ray computed tomography imaging. JACS, 2007. 129(24): p. 7661-7665. Kim D, Park S, Lee JH, Jeong YY, Jon S. Antibiofouling polymer-coated gold nanoparticles as a contrast agent for in vivo X-ray computed tomography imaging. Journal of the American Chemical Society. 2007 Jun 20;129(24):7661-5.
19. Hu, Y., et al., Multifunctional Fe 3 O 4@ Au core/shell nanostars: a unique platform for multimode imaging and photothermal therapy of tumors. Sci. Rep., 2016. 6(1): p. 1-12. Hu Y, Wang R, Wang S, Ding L, Li J, Luo Y, Wang X, Shen M, Shi X. Multifunctional Fe3O4@ Au core/shell nanostars: a unique platform for multimode imaging and photothermal therapy of tumors. Scientific reports. 2016 Jun 21;6(1):1-2.